

# Probing the Nuclear Equation of State in the quasi-elastic nucleus-nucleus scattering

Dao T. Khoa <sup>a</sup>, W. von Oertzen <sup>b</sup>, H.G. Bohlen <sup>b</sup> and H.S. Than <sup>a</sup>

<sup>a</sup>*Institute for Nuclear Science and Technique, P.O. Box 5T-160, Nghia Do, Hanoi, Vietnam.*

<sup>b</sup>*Hahn-Meitner-Institut Berlin GmbH, Glienicker Str. 100, D-14109 Berlin, Germany.*

Large-angle elastic scattering of  $\alpha$ -particle and strongly-bound light nuclei at a few tens MeV/nucleon has shown the pattern of *rainbow scattering*. This interesting process was shown to involve a significant overlap of the two colliding nuclei, with the total nuclear density well above the saturation density of normal nuclear matter (NM). For a microscopic calculation of the nucleus-nucleus potential within the folding model, we have developed a *density dependent* nucleon-nucleon (NN) interaction based on the G-matrix interaction M3Y. Our folding analysis of the refractive  $^4\text{He}$ ,  $^{12}\text{C}$ , and  $^{16}\text{O}$  elastic scattering shows consistently that the NM incompressibility  $K$  should be around 250 MeV which implies a rather *soft* nuclear Equation of State (EOS). To probe the symmetry part of the nuclear EOS, we have used the isovector coupling to link the isospin dependence of the proton optical potential to the cross section of  $(p, n)$  charge-exchange reactions exciting the isobaric analog states in nuclei of different mass regions. With the isospin dependence of the NN interaction fine tuned to reproduce the charge exchange data, a realistic estimate of the NM symmetry energy has been made.

## 1 What is the nuclear rainbow?

The atmospheric rainbow is observed in nature whenever there are water droplets illuminated by the sun light. It can be seen during the rain with the sunshine not completely covered by the clouds or from a fountain when the sunlight enters from behind the point of observation. Beside the fascinating effect of color splitting in the rainbow caused by the dependence of the refraction index on the light wavelength, a physically more interesting effect is the *increased* light intensity around the rainbow angle  $\Theta_R$  and the *shadow* region lying beyond  $\Theta_R$  which are results of a particular refraction - reflection sequence.

Although Descartes has successfully explained the origin of the atmospheric rainbow based on simple geometrical ray optics in 1637, neither he nor Newton and Young (several decades later) could explain the fine structure of the rainbow seen as the *supernumeraries* (the faint bows located just below the primary bow). The first complete mathematical description of the atmospheric rainbow was given in 1838 by Airy, and the oscillation of the light intensity near the rainbow angle is now known as Airy oscillation which

gives rise to the supernumeraries. As nuclei are approximately spherical objects (like water drops) having wave properties, they can be refracted or undergo interference in the nucleus-nucleus scattering, like the refraction of sunlight by the water drops. As a result, one may observe phenomena like rainbow in the nuclear scattering if the conditions are right. Indeed, the rainbow pattern was clearly observed in large-angle elastic scattering of  $\alpha$ -particles and some strongly-bound light nuclei at few tens MeV/nucleon, where signatures of the Airy oscillation pattern has been identified. An important feature of the nuclear rainbow is that it allows us to probe the nucleus-nucleus interaction at small distances [1] thanks to a *weak* absorption in the nucleus-nucleus system.

## 2 From nuclear rainbow to the equation of state for cold nuclear matter

For a microscopic description of the elastic nucleus-nucleus scattering, the folding model analysis is usually performed, where the (real) nucleus-nucleus optical potential is calculated as a Hartree-Fock (HF) potential of the dinuclear system [2,3] using an effective

nucleon-nucleon (NN) interaction [4]

$$V = \sum_{ij} [\langle ij | v_D | ij \rangle + \langle ij | v_{EX} | ji \rangle], \quad (1)$$

where  $|i\rangle$  and  $|j\rangle$  are the single-particle wave functions of nucleons in the two colliding nuclei  $A_1$  and  $A_2$ , respectively;  $v_D$  and  $v_{EX}$  are the direct and exchange parts of the effective NN interaction. It turns out that the density dependence of the effective NN interaction can be accurately tested in the folding analysis of the refractive elastic  $\alpha$ -nucleus or nucleus-nucleus scattering data [2,5]. For this purpose, a phenomenological density dependence was first introduced to the M3Y interaction based on the G-matrix elements of the Reid and Paris NN potentials [6], to reproduce the saturation properties of cold nuclear matter (NM) in the HF scheme [4]. From the HF results for the NM energy (per nucleon) plotted in Fig. 1, one can see that different sets of the density dependence give values of the NM *incompressibility*  $K$  ranging from 170 to above 500 MeV. Since the  $K$  value is a key input in the NM equation of state (EOS), a test of the density dependence of the NN interaction is also an indirect test of the nuclear EOS. In the elastic channel, the two colliding nuclei remain in the ground state (g.s.) even when they overlap strongly at small impact parameters, since any density deformation or rearrangement directly projects the system out of the elastic channel. Therefore, the total density  $\rho$  of the two overlapping nuclei which enters Eq. (1) must be taken as the sum of the two g.s. densities and the total density for a projectile overlapping a target nucleus may reach as much as twice the normal NM density  $\rho_0$  [1,2]. Note that the shorter the impact parameter the higher the overlap density and the more the nucleus-nucleus potential becomes sensitive to the density dependence of the NN interaction. At small impact parameters (or low partial waves) the survival probability of the elastic wave is usually less than 1% and requires, therefore, a very precise measurement of elastic events at large scattering angles. These large-angle data points give

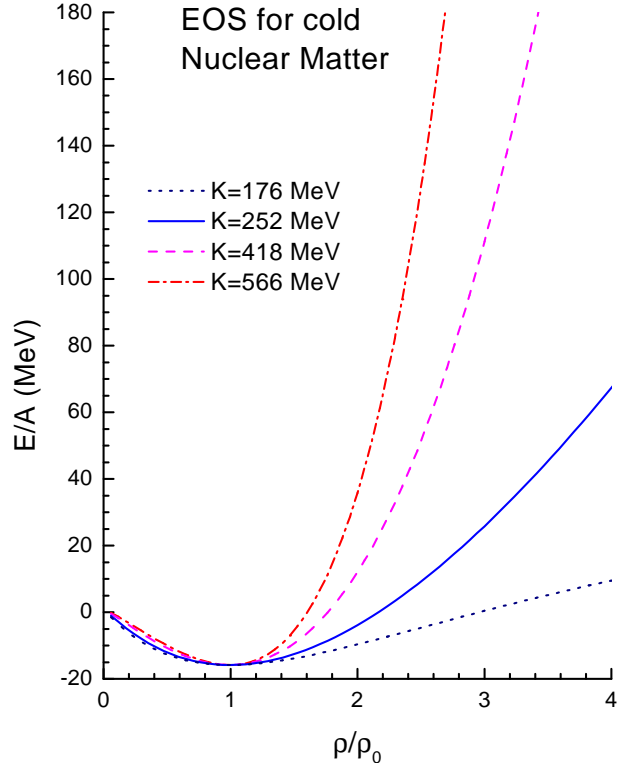


Fig. 1. EOS for cold NM given by the HF calculation using different density dependent NN interactions (which give different values of the NM incompressibility  $K$ ).

us the most vital information about the reliability of the effective NN interaction used in the folding calculation [8]. From results of the folding analysis of the elastic  $^{16}\text{O}+^{16}\text{O}$  scattering data at 350 MeV [7] plotted in Fig. 2 one can clearly see which is the most appropriate density dependence of the NN interaction (in the corresponding  $K$  value). Together with the results obtained earlier for elastic scattering of  $\alpha$  particles and other light projectiles [8], we conclude that the most realistic value for the NM incompressibility  $K$  is around 230 - 270 MeV which corresponds to a rather *soft* EOS. We stress that the broad bump seen in Fig. 2 at  $\Theta_{\text{c.m.}} \approx 50^\circ$  has been specified as the first Airy maximum [9], and the observed rainbow pattern is quite sensitive to the  $^{16}\text{O}+^{16}\text{O}$  optical potential at small distances. It can be shown for the considered  $^{16}\text{O}+^{16}\text{O}$  system (see Fig. 3) that the large-angle data are sensitive to the impact parameters as small as 2 fm. At such small internuclear distances, the total overlap density of the system reaches up to  $2\rho_0$

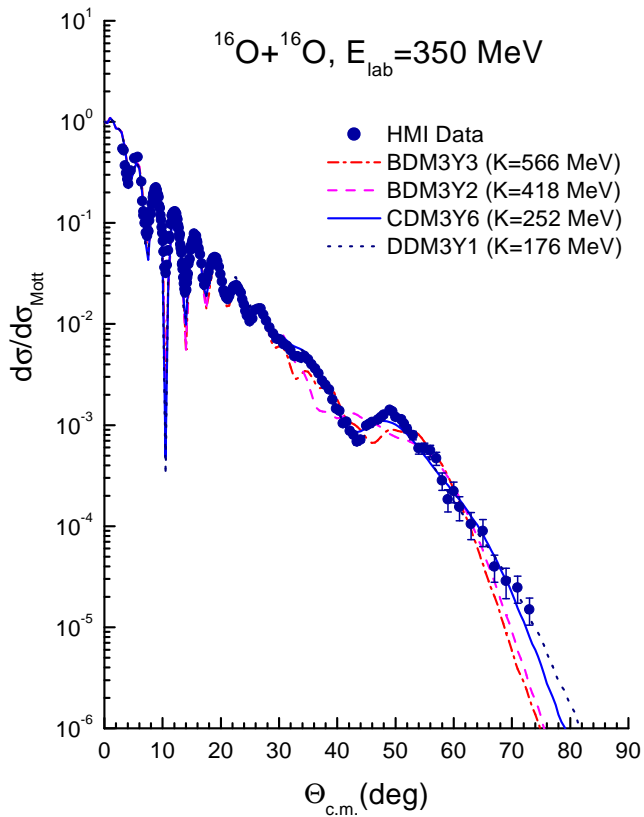


Fig. 2. Folding model description of the elastic  $^{16}\text{O}+^{16}\text{O}$  scattering data at  $E_{\text{lab}} = 350$  MeV [7], using the same density dependent NN interactions as those in Fig. 1. The best-fit interaction is CDM3Y6 which gives  $K \approx 252$  MeV.

[8]. Therefore, the elastic refractive nucleus-nucleus scattering data like those measured for the  $^{16}\text{O}+^{16}\text{O}$  system at 350 MeV provide a very good data base for probing the high overlap density in the elastic channel.

### 3 Probing EOS of the asymmetric NM via charge-exchange reaction

The nuclear EOS presented in Fig. 1 was obtained in a HF calculation for symmetric NM, i.e., with equal proton and neutron densities. In reality, the NM that exists in the neutron stars is highly asymmetric, with the neutrons outnumbering protons by factor of about 2 in the crust of a neutron star. Therefore, the knowledge about the symmetry part of the EOS is vital for the understanding of the dynamics of supernovae explosion and the formation of neutron stars [10,11]. The symmetry part of the nuclear EOS is determined essentially by the NM symmetry energy  $S(\rho)$  (defined in terms of a Taylor series expansion

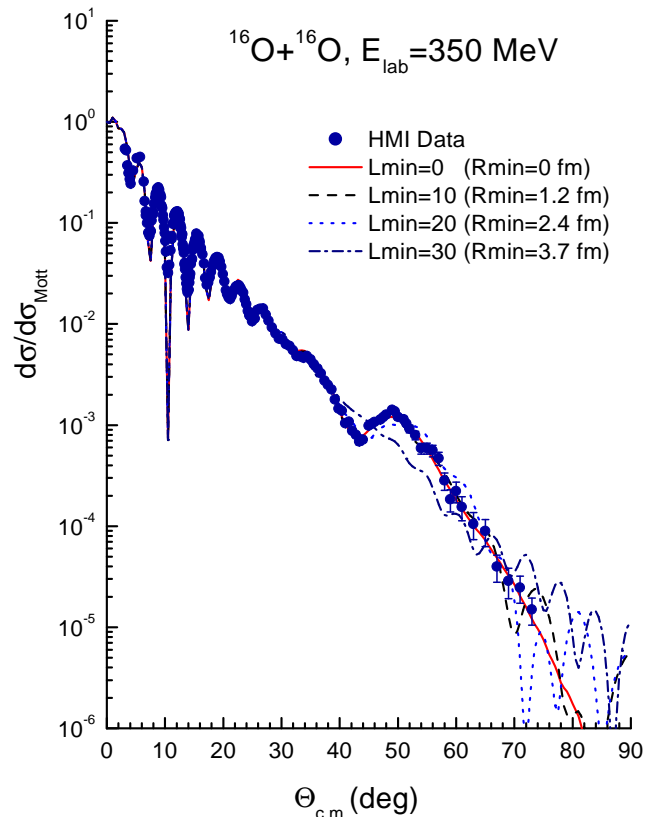


Fig. 3. The same description as in Fig. 2 given by the CDM3Y6 interaction, but with different cutoff values of the lowest partial wave  $L_{\text{min}}$  (and the corresponding impact parameters  $R_{\text{min}}$ ).

of the NM binding energy  $B \equiv E/A$  as

$$B(\rho, \delta) = B(\rho, 0) + S(\rho)\delta^2 + O(\delta^4) + \dots \quad (2)$$

where  $\delta = (\rho_n - \rho_p)/\rho$  is the neutron-proton asymmetry parameter. The contribution of  $O(\delta^4)$  and higher-order terms in Eq. (2), i.e., the deviation from the parabolic law was proven to be negligible [12]. The NM symmetry energy determined at the NM saturation density,  $E_{\text{sym}} = S(\rho_0)$  with  $\rho_0 \approx 0.17 \text{ fm}^{-3}$ , is widely known in the literature as the *symmetry energy* or symmetry coefficient. Although numerous nuclear many-body calculations have predicted  $E_{\text{sym}}$  to be around 30 MeV, a direct experimental determination of  $E_{\text{sym}}$  still remains a challenging task. One needs, therefore, to relate  $E_{\text{sym}}$  to some experimentally inferable quantity like the neutron skin in neutron-rich nuclei [13] or the fragmentation data of heavy-ion (HI) collisions involving  $N \neq Z$  nuclei [14]. Within the frame of any microscopic model for asymmetric NM, the symmetry energy depends strongly on

the isospin dependence of the NN interaction used therein [12]. Therefore, the  $E_{\text{sym}}$  value can be indirectly tested in a charge exchange (isospin-flip) reaction which has been known for decades as a good probe of the isospin dependence of the effective NN interaction [15]. Although the isospin dependence of the nuclear optical potential (OP), known by now as Lane potential [16], has been studied since a long time, there has been a considerable interest recently in studying the isospin dependence of the OP in the quasi-elastic scattering reactions measured with unstable neutron-rich beams. Based on the isospin symmetry, the nucleus-nucleus OP can be written in terms of an isovector coupling [16] as

$$U(R) = U_0(R) + 4U_1(R)\frac{\mathbf{t}\cdot\mathbf{T}}{aA}, \quad (3)$$

where  $\mathbf{t}$  is the isospin of the projectile  $a$  and  $\mathbf{T}$  is that of the target  $A$ . While the relative contribution by the Lane potential  $U_1$  to the elastic  $(p, p)$  cross section is small and amounts only to a few percent for a neutron-rich target, it determines entirely the (Fermi-type)  $\Delta J^\pi = 0^+$  transition strength of the  $(p, n)$  reaction leading to an isobaric analog state (IAS). Therefore, the  $(p, n)$  reaction has been so far the main tool in studying the isospin dependence of the proton-nucleus OP. Since this isospin dependence should be better tested in the charge exchange reactions induced by the neutron-rich beams, we consider in the present work the  $p(^6\text{He}, ^6\text{Li}^*)n$  reaction measured by Cortina-Gil *et al.* [17] with the secondary  $^6\text{He}$  beam at  $E_{\text{lab}} = 41.6A$  MeV. Given a large neutron-proton asymmetry ( $\delta = 1/3$ ) of the unstable  $^6\text{He}$  nucleus, the measured  $p(^6\text{He}, ^6\text{Li}^*)n$  cross section for the transition connecting the ground state of  $^6\text{He}$  ( $T = T_z = 1$ ) and its isobaric analog partner ( $T = 1, T_z = 0, J^\pi = 0^+$  excited state of  $^6\text{Li}$  at 3.563 MeV) is indeed a good probe of the isovector coupling in the  $^6\text{He}+p$  system. To link the Lane potential  $U_1$  to the isospin dependence of the NN interaction, we have used the folding model [18] to calculate  $U_0$  and  $U_1$  using the explicit proton and neutron g.s. densities of  $^6\text{He}$  and the

CDM3Y6 density- and isospin dependent NN interaction [8]. The only nuclear structure input is the  $^6\text{He}_{\text{g.s.}}$  density and we have used the microscopic density given by the cluster-orbital shell model approximation (COSMA) [19]. The  $p(^6\text{He}, ^6\text{Li}^*)n$  cross sections given

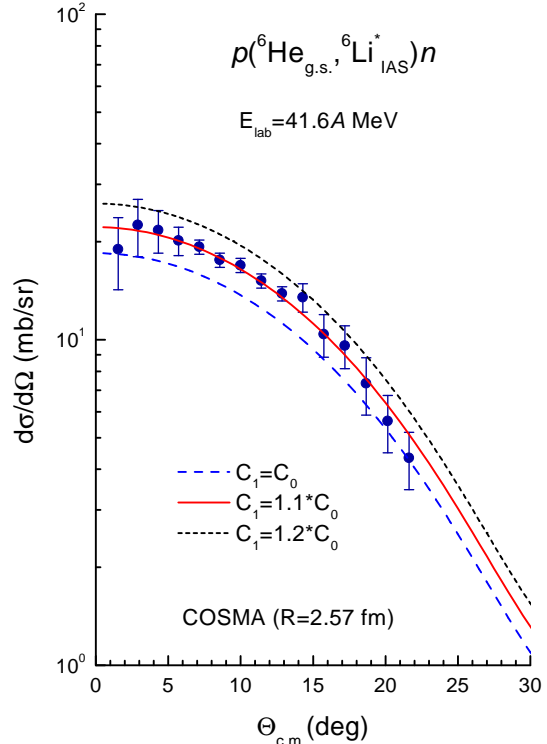


Fig. 4. CC results for the charge exchange  $p(^6\text{He}, ^6\text{Li}^*)n$  cross section at  $E_{\text{lab}} = 41.6A$  MeV in comparison with the data measured by Cortina-Gil *et al.* [17].

by the coupled-channel (CC) calculation using a charge-exchange form factor based on the Lane potential  $U_1$  were found to have a shape very close to that of the measured angular distribution (see Fig. 4). Since the complex strength of the form factor was fixed by the folding model analysis of the elastic  $^6\text{He}+p$  scattering [20], the CC description of the  $p(^6\text{He}, ^6\text{Li}^*)n$  data could be improved only by fine tuning the strength  $C_1$  of the isovector part of the density dependence of the CDM3Y6 interaction [12]. One can see that the best fit is achieved when  $C_1$  is about 10% stronger than the isoscalar strength  $C_0$ . To make a more definitive conclusion on the EOS of asymmetric NM, we found it neces-

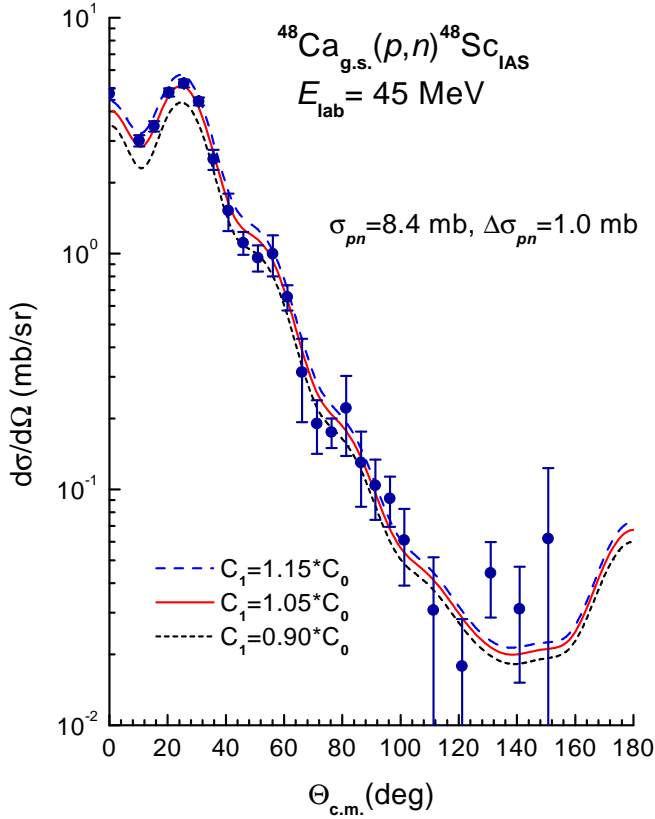


Fig. 5. CC results for the charge exchange  $^{48}\text{Ca}(p,n)^{48}\text{Sc}$  cross section at the incident proton energy of 45 MeV in comparison with the data measured by Doering *et al.* [15].

sary to make a systematic folding analysis of the charge exchange ( $p, n$ ) reactions measured with targets in different mass regions. Therefore, the same density- and isospin dependent NN interaction has been used to construct the charge exchange form factors for the ( $p, n$ ) reactions measured at the incident proton energies of 35 and 45 MeV with the targets  $^{48}\text{Ca}$ ,  $^{90}\text{Zr}$ ,  $^{120}\text{Sn}$  and  $^{208}\text{Pb}$  [15]. Although the neutron-proton asymmetry  $\delta$  of these nuclei is smaller than that of unstable  $^6\text{He}$  nucleus, the complex proton OP for these nuclei has been studied over the years [21] and, hence, it allows us to unambiguously probe the isovector part of the OP via the ( $p, n$ ) reaction. By using a most appropriate complex proton OP which produces not only the elastic scattering data but also the polarization data and the experimental total reaction cross section for each of the considered targets, we have come up with about the same accurate description of the ( $p, n$ ) reactions leading to the excitation of IAS in  $^{48}\text{Ca}$ ,  $^{90}\text{Zr}$ ,  $^{120}\text{Sn}$  and  $^{208}\text{Pb}$  as that

presented above for the unstable  $^6\text{He}$ . Our CC results for the charge exchange  $^{48}\text{Ca}(p,n)^{48}\text{Sc}$  cross section at 45 MeV and the data measured by Doering *et al.* [15] are shown in Fig. 5 as an illustration of the success of our approach. The best-fit isovector strength  $C_1$  of the CDM3Y6 interaction was adjusted in each case not only to reproduce the measured angular distribution for the considered ( $p, n$ ) reaction but also to obtain the measured *total* ( $p, n$ ) cross section in our CC calculation. For example, the  $C_1$  values used to calculate the  $^{48}\text{Ca}(p,n)^{48}\text{Sc}$  cross section shown in Fig. 5 was constrained by a CC calculation giving the experimental total  $^{48}\text{Ca}(p,n)^{48}\text{Sc}$  cross section of  $8.4 \pm 1.0$  mb [15]. If one takes into

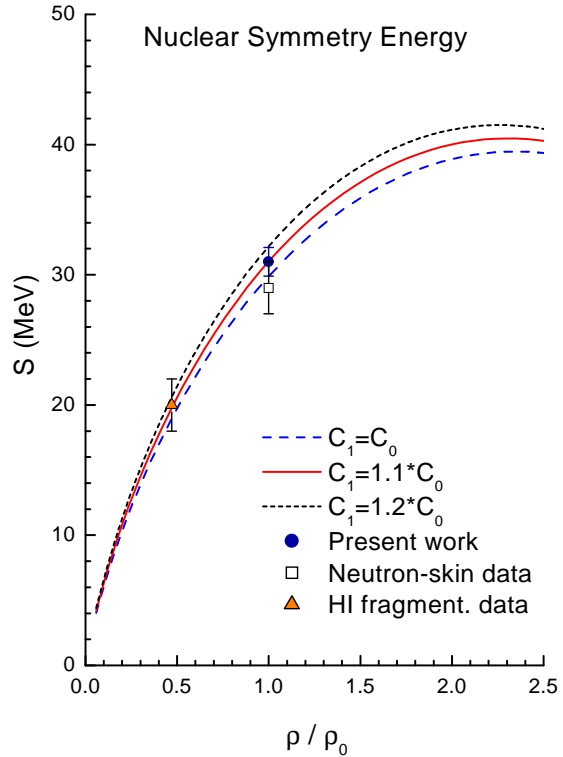


Fig. 6. Density dependence of the NM symmetry energy  $S(\rho)$  predicted by the HF formalism [12] using the same isovector strengths  $C_1$  as those used in Fig. 4 and the (empirical) neutron-skin [13] and HI fragmentation [14] data.

account only the uncertainty of the measured ( $p, n$ ) angular distribution, the range of acceptance for  $C_1$  values becomes significantly larger. Given the results of our CC calculation of the ( $p, n$ ) reactions for  $^{48}\text{Ca}$ ,  $^{90}\text{Zr}$ ,

$^{120}\text{Sn}$  and  $^{208}\text{Pb}$  [22], we conclude that the best-fit isovector strength  $C_1$  of the CDM3Y6 interaction is slightly larger than the isoscalar strength  $C_0$ , with about the same uncertainty as that found in the analysis of  $p(^6\text{He}, ^6\text{Li}^*)n$  reaction.

With the isovector strength of the CDM3Y6 interaction now well tested, we have further performed the HF calculation [12] of asymmetric NM using this same isospin- and density dependent interaction. The density dependence of the NM symmetry energy  $S(\rho)$  obtained with the same isovector strengths  $C_1$  as those used in Fig. 4 is shown in Fig. 6, and one can deduce easily  $E_{\text{sym}} \approx 31 \pm 1$  MeV from our HF results. This result is quite complementary to the structure studies which relate the  $E_{\text{sym}}$  value to the neutron skin, a method first suggested by Brown [23]. If one adopts a neutron-skin  $\Delta R \approx 0.1 - 0.2$  fm for  $^{208}\text{Pb}$  then a systematics based on the mean-field calculations [13] gives  $E_{\text{sym}} \approx 27 - 31$  MeV (which is plotted in Fig. 6). Our result is also complementary to the recent studies of HI fragmentation based on the antisymmetrized molecular dynamics [14] which obtained  $S(\rho \approx 0.08 \text{ fm}^{-3}) \approx 18 - 22$  MeV at a *finite* temperature around 3 MeV. If we neglect the temperature dependence of  $S(\rho)$  at low NM densities, this value turns out to agree well with our HF result for the low-density part of  $S(\rho)$  as shown in Fig. 6.

In conclusion, the charge exchange reaction like  $(p, n)$  or  $(^3\text{He}, t)$  should be a very powerful tool in studying not only the nuclear structure but also the isospin aspects of the EOS for asymmetric NM.

#### 4 Acknowledgement

This work has been supported, in part, by the Natural Science Council of Vietnam, A.v. Humboldt Stiftung of Germany, EU Asia-Link Program CN/Asia-Link/008 (94791) and Vietnam Atomic Energy Commission.

#### References

[1] W. von Oertzen, D.T. Khoa and H.G. Bohlen, *Europhysicsnews* 31(2), 2000, 5;

31(3), 2000, 21.  
 [2] D.T. Khoa, W. von Oertzen and H.G. Bohlen, *Phys. Rev. C* 49, 1994, 1652.  
 [3] M.E. Brandan and G.R. Satchler, *Phys. Rep.* 285, 1997, 143.  
 [4] D.T. Khoa and W. von Oertzen, *Phys. Lett. B* 304, 1993, 8; *Phys. Lett. B* 342, 1995, 6.  
 [5] D.T. Khoa *et al.*, *Phys. Rev. Lett.* 74, 1995, 34.  
 [6] G. Bertsch *et al.*, *Nucl. Phys. A* 284, 1977, 399; N. Anantaraman, H. Toki and G. Bertsch, *Nucl. Phys. A* 398, 1983, 269.  
 [7] E. Stiliaris *et al.* *Phys. Lett. B* 223, 1989, 291.  
 [8] D.T. Khoa, G.R. Satchler and W. von Oertzen, *Phys. Rev. C* 56, 1997, 954.  
 [9] D.T. Khoa, W. von Oertzen, H.G. Bohlen and F. Nuoffer, *Nucl. Phys. A* 672, 2000, 387.  
 [10] H.A. Bethe, *Rev. Mod. Phys.* 62, 1990, 801.  
 [11] F.D. Swesty, J.M. Lattimer and E.S. Myra, *Astrophys. J.* 425, 1994, 195.  
 [12] D.T. Khoa, W. von Oertzen and A. A. Ogloblin, *Nucl. Phys. A* 602, 1996, 98.  
 [13] R.J. Furnstahl, *Nucl. Phys. A* 706, 2002, 85.  
 [14] A. Ono *et al.*, *Phys. Rev. C* 70, 2004, 041604(R); D.V. Shetty *et al.* *Phys. Rev. C* 70, 2004, 011601(R).  
 [15] R.R. Doering, D.M. Patterson and A. Galonsky, *Phys. Rev. C* 12, 1975, 378.  
 [16] A.M. Lane, *Phys. Rev. Lett.* 8, 1962, 171.  
 [17] M.D. Cortina-Gil *et al.*, *Nucl. Phys. A* 641, 1998, 263.  
 [18] D.T. Khoa, E. Khan, G. Colò and N.V. Giai, *Nucl. Phys. A* 706, 2002, 61.  
 [19] A.A. Korshennikov *et al.*, *Nucl. Phys. A* 617, 1997, 45.  
 [20] D.T. Khoa and H.S. Than, *Phys. Rev. C* 71, 2005, 044601.  
 [21] R.L. Varner *et al.*, *Phys. Rep.* 201, 1991, 57.  
 [22] D.T. Khoa *et al.*, to be submitted.  
 [23] B.A. Brown, *Phys. Rev. Lett.* 85, 2000, 5296.